An Inverse Approach for Determining Creep Properties from a Miniature Thin Plate Specimen under Bending

Y. Zheng, W. Sun

Abstract—This paper describes a new approach which can be used to interpret the experimental creep deformation data obtained from miniaturized thin plate bending specimen test to the corresponding uniaxial data based on an inversed application of the reference stress method. The geometry of the thin plate is fully defined by the span of the support, l, the width, b, and the thickness, d. Firstly, analytical solutions for the steady-state, load-line creep deformation rate of the thin plates for a Norton's power law under plane stress ($b\rightarrow0$) and plane strain ($b\rightarrow\infty$) conditions were obtained, from which it can be seen that the load-line deformation rate of the thin plate under plane-stress conditions is much higher than that under the plane-strain conditions. Since analytical solution is not available for the plates with random b-values, finite element (FE) analyses are used to obtain the solutions. Based on the FE results obtained for various b/l ratios and creep exponent, n, as well as the analytical solutions under plane stress and plane strain conditions, an approximate, numerical solutions for the deformation rate are obtained by curve fitting. Using these solutions, a reference stress method is utilised to establish the conversion relationships between the applied load and the equivalent uniaxial stress and between the creep deformations of thin plate and the equivalent uniaxial creep strains. Finally, the accuracy of the empirical solution was assessed by using a set of "theoretical" experimental data.

Keywords—Bending, Creep, Miniature Specimen, Thin Plate.

I. INTRODUCTION

POWER plants and chemical plants may operate at elevated temperatures for extended periods of time, e.g. more than 30 years. During this time, the material used in the construction of the plants degrades and the creep strength of the material reduces. NDT and small specimen test techniques can be employed to sample and test the material. For this reason, various small or miniature specimen test methods have been developed and used [1]. The latest work on small specimen creep testing involves the development of specimen types which are suitable for obtaining creep strain rate and creep rupture data [2]. The small test specimens used for these types of tests can be obtained from small button-shaped (scoop) samples, which are removed, for example, by a non-destructive sampling technique [3].

Small specimen creep testing has become increasingly attractive for power plant applications because some power plant components are now operating beyond their original design life, and economic, "non-invasive" and reliable testing techniques are required when performing remaining life evaluations [3]. Data from small volumes of materials have a direct input into remaining life and ranking studies, thereby improving the confidence of plant/component life prediction and managing the potential risk [4]. Such data can also be used to generate creep constitutive laws for weld materials and for local heated-affected zone structures generated during the welding process [5].

The main small specimen types that are used to obtain creep properties include the conventional sub-size uniaxial specimens [6] and several specialised miniature specimen types including: the impression specimen [7], [8], Fig. 1 (a), the small punch specimen [9], [10], Fig. 1 (b), the small ring specimen [11], [12], Fig. 1 (c), and the small tensile bar specimen [13], Fig. 1 (d). One of the unique advantages the small punch creep test has is that one of the specimen dimensions (the thickness) is very small (0.3 to 0.5mm), however, up to date, there are no universally accepted conversion techniques available for data interpretation, due to its complicated deformation and failure mechanisms [10]. Previous research has been carried out using miniaturised beam on pure bending specimen type [14]. This paper describes a technique which can be used to interpret the experimental creep deformation data obtained from miniaturized thin plate bending specimen test to the corresponding uniaxial data based on an inversed application of the reference stress method.
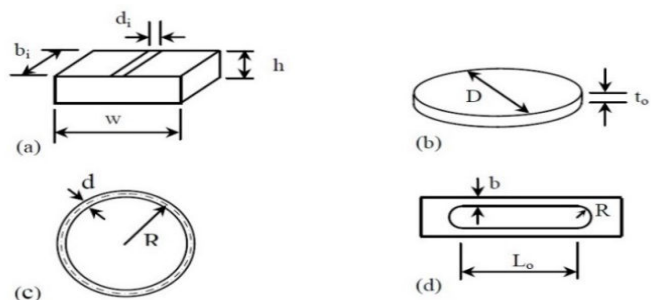
Y. Zheng was with the Department of Mechanical, Materials and Manufacturing Engineering at University of Nottingham, UK and now is with Department of Mechanical Engineering at Imperial College London, UK (e-mail: zhengyang1991@gmail.com).

W. Sun is a Professor in the Department of Mechanical, Materials and Manufacturing Engineering at University of Nottingham, UK (phone: +44 115 9513809; e-mail:w.sun@nottingham.ac.uk; fax: +44 115 9513800).

Fig. 1 Small creep test specimens: (a) Impression; (b) Small punch; (c) Small ring; and (d) Small bar type

II. ANALYTICAL SOLUTIONS FOR STEADY-STATE CREEP DEFORMATION RATES

A. Norton's Law

Norton's Law is the most common material behaviour model to describe the steady-state creep of bulk deformation behaviour. The multi-axial form of the Norton's law is given by:

$$\dot{\varepsilon}_{eq}^c = B\sigma_{eq}^n \tag{1}$$

where B is the creep resistant coefficient and n is the stress index. The individual components of the creep strain rates are given by:

$$\dot{\varepsilon}_{ij}^c = \frac{3}{2}B\sigma_{eq}^n\left(\frac{S_{ij}}{\sigma_{eq}}\right) \tag{2}$$

The uniaxial form of the Norton's law is:

$$\dot{\varepsilon}^c = B\sigma^n \tag{3}$$

B. Analytical Solutions under Plane Stress Conditions

A thin rectangular plate with simple supports subjected to a vertical force P in the middle is illustrated in Fig. 2. Since the plate is thin, the effect of the shear stress contribution and the stress in the thickness direction are assumed to be negligible. Under the plane stress conditions, the plate is treated as a beam under pure bending, where the stress state of the plate is uniaxial. Detailed derivation procedure using a complementary strain energy approach can be seen in Appendix A. The load line direction steady-state creep deformation rate of the thin plate under the plane stress conditions is:

$$\dot{\Delta}_{ss}^c = \left(\frac{2n+1}{2n}\right)^n\frac{1}{2(n+2)}\cdot\frac{l^2}{d}\cdot B\left(\frac{Pl}{bd^2}\right)^n \tag{4}$$
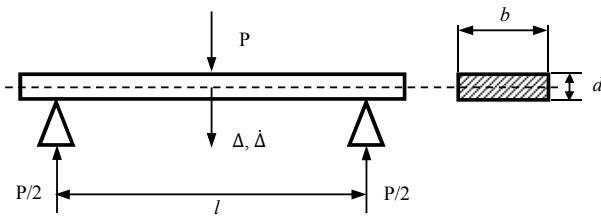

Fig. 2 Schematics of the three-point bending model (plane stress)

C. Analytical Solutions under Plane Strain Conditions

As shown in Fig. 3, a thin plate with simple supports is subjected to a vertical line force $\bar{p}$ in the middle. Since the thickness of the plate is small compared to its length and width, the stress in z direction is assumed to be negligible ($\sigma_z = 0$). Therefore, under the plane strain condition ($\varepsilon_y = 0$), the stress state in the plate is bi-axial. The load line direction steady-state creep deformation rate of the thin plate under the plane strain ($b\rightarrow\infty$) conditions is:

$$\dot{\Delta}_{ss}^c = \left(\frac{2n+1}{2n}\right)^n\frac{1}{2(n+2)}\cdot\frac{3^{\frac{n+1}{2}}}{4}\frac{l^2}{d}\cdot B\left(\frac{\bar{p}l}{d^2}\right)^n \tag{5}$$

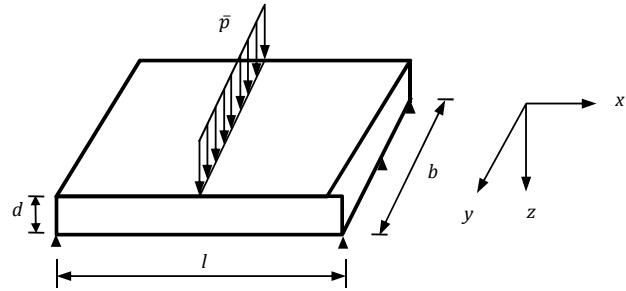Detailed derivation procedure can be seen in Appendix B.

Fig. 3 Schematics of the three point bending model

III. APPROXIMATE, EMPIRICAL SOLUTION FOR STEADY-STATE CREEP DEFORMATION RATES

A. Finite Element Analysis

Finite element analyses for the thin plate under three-point bending were performed to verify the 2D analytical solutions, and to produce the numerical results for steady-state deformation rate for various b/l ratios between the plane stress and plane strain. Under a given support condition, the load-line direction steady-state creep deformation rate of the plate is related to the Norton's constants, B and n, and the plate geometry, i.e. d/l and b/l, see Fig. 3. It is assumed that when d/l is sufficiently small, the shear contribution is negligible, therefore, the deformation solution will be very close to that of pure bending, where the dimension can be characterised by b/l only. In all FE analyses, $d = 1.6$ and $l = 20$ mm are used here although other values of the dimensions can also be used.

B. 2D Plane Stress and Plane Strain Analyses

The variations of load-line creep deformation rate with time under plane stress and plane strain conditions, obtained from 2D FE analyses are shown in Fig. 4. The analyses were performed using plane stress and plane stress elements, with B $= 1.0\times10^{-22}$ (for stress in MPa and time in hour), $n = 6$, and $\bar{p} = 25$ N/m. The results are normalised by the analytical plane strain solutions by using (5) and the t is normalised by t_0 which is the time when "steady-state" is achieved in the FE analysis.

Due to the stress re-distribution in the early stage of creep, the creep deformation rates reduce with time, and become practically un-changed with time (steady-state) when the time is sufficiently long. These "constant" steady-state values of the FE solution are compared with the corresponding analytical solutions from (4) and (5) in Fig. 4.

It can be seen that the steady-state FE solutions are almost identical to the corresponding analytical solutions. In addition, it clearly shows that the deformation rate under plane-stress condition is almost three times of that under plane-strain conditions for $n = 6$. Since the analytical solutions cannot be obtained for random b/l values, 3D FE analyses are used to produce approximate, numerical solutions for these.
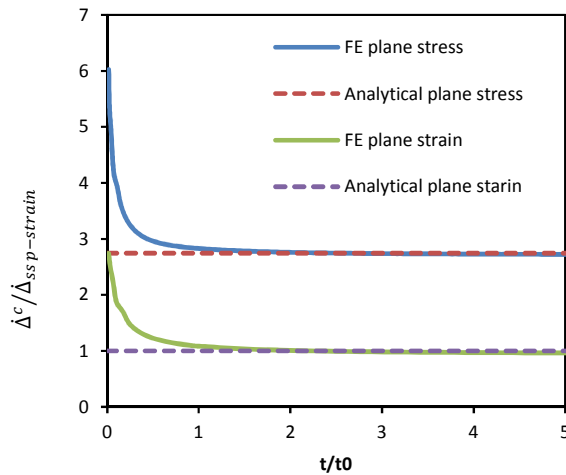
Fig. 4 Comparison of analytical and FE creep deformation rates under plane stress and plane strain conditions (B = 1.0×10^{-22}, n = 6, and $\bar{p}$ = 25 N/m. l = 20 mm and d = 1.6 mm)

C. 3D Results for a Range of n and b/l

To evaluate the deformation rate under 3D conditions, FE analyses were performed subjected to a constant line load of $\bar{p}$ = 25 N/m, with b/l varying from 0.25 to 5. In all cases, l = 20mm and d = 1.6mm were used. The normalised results for B = 1.0×10^{-22} and n = 6 are plotted in Fig. 5.

It can be seen from Fig. 5 that the steady-state creep deformation rate reduce with the increase of the b/l ratio, and this reduction become less significant as the b/l ratio becomes larger. When b/l is less than ~ 0.1 (the plate can be regarded as a thin beam), the FE results are very close to that for plane stress, and when b/l is great than ~ 2.5, the results are very close to that for plane-strain. Since the variation with b/l is relatively simple, curve or surface fitting is assumed to be reasonable to be used to derive an empirical solution of the load-line steady-state deformation rate as a function of b/l and n.
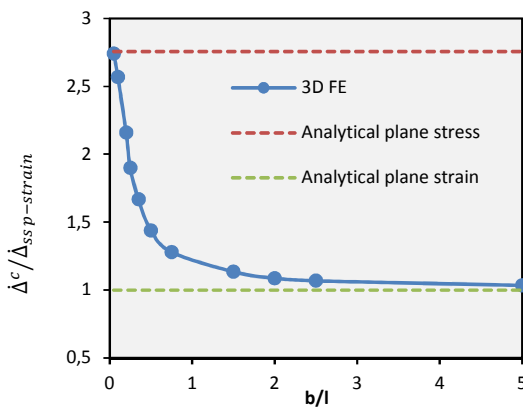

Fig. 5 Variation of normalised steady-state deformation rates with b/l obtained from FE analyses (n = 6)

The analyses similar to those shown in Fig. 5 were conducted with other n-values varying from 2 to 10. The results obtained are shown in Fig. 6, from which it can be seen that a relatively smooth surface was obtained.
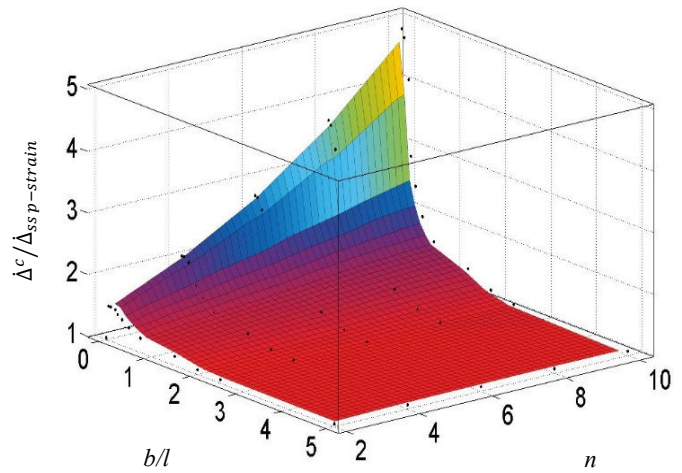

Fig. 6 Surface fitting to the normalised steady-state creep deformation rate plot with b/l and n

D. Fitting Functions between Plane Stress and Plane Strain

In order to obtain a suitable b/l and n dependent function by fitting the 3D FE results, for the same n-value, the FE steady-state creep deformation rate results are normalised by the corresponding result for plane strain. The function of the surface is found to be hard to be expressed by a single polynomial function. In order to reduce the error, the numerical empirical solutions of the surface are determined separately with respect to different b/l regions, see (6)-(9).

For $0.25 < b/l < 0.45$:

$$f\left(\frac{b}{l}, n\right) = 1.469 - 2.237\left(\frac{b}{l}\right) - 0.26n + 4.846\left(\frac{b}{l}\right)^2 - 0.6455n\left(\frac{b}{l}\right) - 0.0002255n^2 - 3.481n\left(\frac{b}{l}\right)^3 + 0.4811n\left(\frac{b}{l}\right)^2 - 0.001068n^2\left(\frac{b}{l}\right) \quad (6)$$

For $0.45 < b/l < 0.75$:

$$f\left(\frac{b}{l}, n\right) = 1.293 - 0.4461\left(\frac{b}{l}\right) + 0.2093n + 0.2646\left(\frac{b}{l}\right)^2 - 0.5017n\left(\frac{b}{l}\right) + 0.002846n^2 + 0.3164n\left(\frac{b}{l}\right)^2 + 0.002915n^2\left(\frac{b}{l}\right) - 0.0003099n^3 \quad (7)$$

For $0.75 < b/l < 1.3$:

$$f\left(\frac{b}{l}, n\right) = 1.273 - 0.3392\left(\frac{b}{l}\right) + 0.0989n + 0.135\left(\frac{b}{l}\right)^2 - 0.1442n\left(\frac{b}{l}\right) + 0.003196n^2 + 0.04933n\left(\frac{b}{l}\right)^2 + 0.0009457n^2\left(\frac{b}{l}\right) - 0.0002605n^3 \quad (8)$$

For $1.3 < b/l < 2$:

$$f\left(\frac{b}{l}, n\right) = 1.202 - 0.1948\left(\frac{b}{l}\right) + 0.04445n + 0.05156\left(\frac{b}{l}\right)^2 - 0.01461n\left(\frac{b}{l}\right) - 0.0005072n^2 \quad (9)$$

TABLE I
ACCURACY OF THE FITTING FUNCTION (6)-(9) FROM TYPICAL CASES

n	b/l	FE	(6)-(9)	Errors (%)
3	1.6	1.086731	1.078	0.790
5	0.3	1.671243	1.643	0.681
9	0.7	1.426226	1.402	1.719

TABLE II
CONVERSION FACTORS FOR DIFFERENT STRESS CONDITIONS OF THE THIN PLATE

Conditions	b/l	β	η	β
P-stress	0	$\left(\frac{2n+1}{2n\eta}\right)^n \cdot \frac{1}{2(n+2)}$	~0.88	~0.230
P-strain	∞	$\left(\frac{2n+1}{2n\eta}\right)^n \cdot \frac{1}{2(n+2)} \cdot \frac{3^{\frac{n+1}{2}}}{4}$	~0.76	~0.198
3D stress	0~∞	$f\left(\frac{b}{l},n\right) \cdot \left(\frac{2n+1}{2n\eta}\right)^n \cdot \frac{1}{2(n+2)} \cdot \frac{3^{\frac{n+1}{2}}}{4}$	Varying with b/l	

In order to evaluate the accuracy, the empirical solutions are compared to the FE analysis results with some random b/l and n values which were not used in the fitting. In general, the errors are less than 1%; higher values of error occur when b/l = 0.7, since the chosen polynomial function cannot perfectly match up with the part of the surface of large gradient. Some typical errors are shown in Table I.

A general solution ($0.25 < b/l < 2$) for steady-state load-line creep deformation rate of thin plate can be given by:

$$\dot{\Delta}_{ss}^c = f\left(\frac{b}{L},n\right)\left(\frac{2n+1}{2n}\right)^n \cdot \frac{1}{2(n+2)} \cdot \frac{3^{\frac{n+1}{2}}}{4} \cdot \frac{l^2}{d} \cdot B\left(\frac{\bar{p}l}{d^2}\right)^n \quad (10)$$

IV. INVERSE APPROACH WITH REFERENCE STRESS METHOD

A. Conversion Relationships

Using Mackenzie's method [15], (10) may be re-written as

$$\dot{\Delta}_{ss}^c = f\left(\frac{b}{L},n\right)\left(\frac{2n+1}{2n\alpha}\right)^n \cdot \frac{1}{2(n+2)} \cdot \frac{3^{\frac{n+1}{2}}}{4} \cdot \frac{l^2}{d} \cdot B\left(\alpha\frac{\bar{p}l}{d^2}\right)^n$$

Evaluating the value of α, where α is a non-dimensional scaling factor, which makes

$$f\left(\frac{b}{L},n\right)\left(\frac{2n+1}{2n\alpha}\right)^n \cdot \frac{1}{2(n+2)} \cdot \frac{3^{\frac{n+1}{2}}}{4} \quad (11)$$

approximately independent of n, leading to $\alpha = \eta$, and $\sigma_{ref} = \eta\sigma_{nom}$ is the so-called reference stress. Now the deformation rate can be expressed by

$$\dot{\Delta}_{ss}^c = \beta \cdot \frac{l^2}{d} \cdot B\left(\sigma_{ref}\right)^n = \beta \cdot \frac{l^2}{d} \cdot \dot{\varepsilon}\left(\sigma_{ref}\right) \quad (12)$$

where

$$\beta = f\left(\frac{b}{l},n\right)\left(\frac{2n+1}{2n\eta}\right)^n \cdot \frac{1}{2(n+2)} \cdot \frac{3^{\frac{n+1}{2}}}{4} \quad (13)$$

and

$$\sigma_{ref} = \eta\sigma_{nom} = \eta\frac{\bar{p}L}{d^2}$$

η and β are conversion factors. Re-arranging (12) gives

$$\dot{\varepsilon}\left(\sigma_{ref}\right) = \dot{\Delta}_{ss}^c / (\beta l^2/d) \quad (14)$$

where $\beta l^2/d$ in fact is the so-called equivalent gauge length (EGL). The conversion factors η and β are shown in Table II.

When evaluating the value of α, which makes β independent of n, leading to $\alpha = \eta$, only choose two random n value is not enough for an accurate results. In 3D stress conditions, η and β are dependent on b/l, and an MATLAB code was used to find the η value through a variety of n values from 2 to 10, having lowest error of β. Thus, the values of the conversation factors, η and β for b/l from 0.25 to 2 can be obtained, as shown in Figs. 7 and 8.
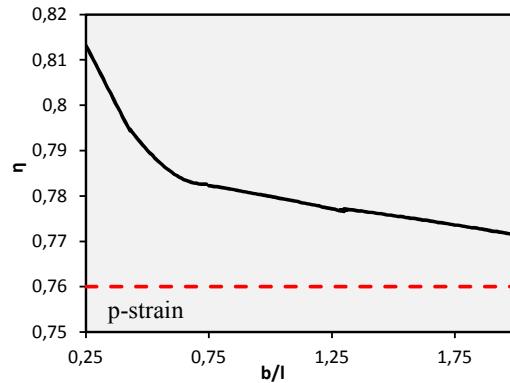
Fig. 7 Variation of conversion factor η with b/l
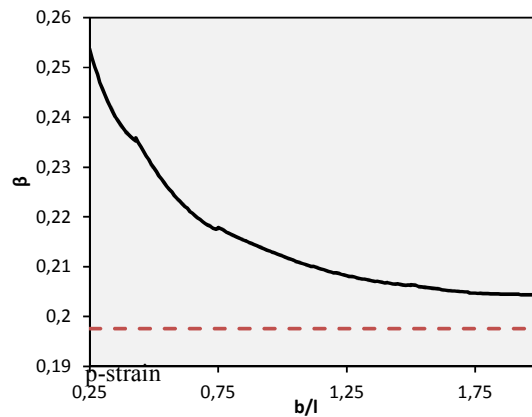
Fig. 8 Variation of conversion factor β with b/l

B. Determination of Creep Properties Using "Theoretical" Experimental Data

A set of "theoretical" experiment tests were performed using FE analysis. The model has a value of $b/l = 0.5$, see Fig. 3, with $l = 20$ mm, $d = 1.6$ mm, B = 1.0×10^{-22} (for stress in MPa and time in hour), $n = 6$, $\beta = 0.23$, and $\bar{p} = 25$ N/m. The equivalent steady-state uniaxial creep strain rate can be given by:

$$\dot{\varepsilon}_{ss}^c\left(\sigma_{ref}\right) = \dot{\Delta}_{ss}^c / (\beta l^2/d)$$

with $b/l = 0.5$, the equation can be re-written as:

$$\dot{\varepsilon}_{ss}^{c}(\sigma_{ref}) = 4.35\dot{\Delta}_{ss}^{c}/(l^2/d)$$

Four load levels are applied on the thin plate, respectively, and based on the equation; the applied load $\bar{p}$ and the steady-state creep deformation rate of the thin plate $\dot{\Delta}_{ss}^{c}$ can be converted to the equivalent uniaxial stress σ_{ref} and the equivalent strain rate, which are shown in Table III.

TABLE III
SIMULATION RESULTS OF THE THIN PLATE

$\bar{p}$ [N/mm]	Δ_{ss}^{c} [mm/h]	σ_{nom} [MPa]	σ_{ref} [MPa]	$\dot{\varepsilon}(\sigma_{ref})$ [h^{-1}]	$\log \sigma_{ref}$	$\log \dot{\varepsilon}(\sigma_{ref})$
20	1.74E-08	156.25	123.453	3.028E-10	2.0915	-9.519
25	6.86E-08	195.31	154.316	1.194E-09	2.1884	-8.923
30	1.97E-07	234.38	185.180	3.428E-09	2.2676	-8.465
35	4.98E-07	273.44	216.043	8.665E-09	2.3345	-8.062

A log-log graph of σ_{ref} and $\dot{\varepsilon}(\sigma_{ref})$ is plotted using the simulated results, as shown in Fig. 9.
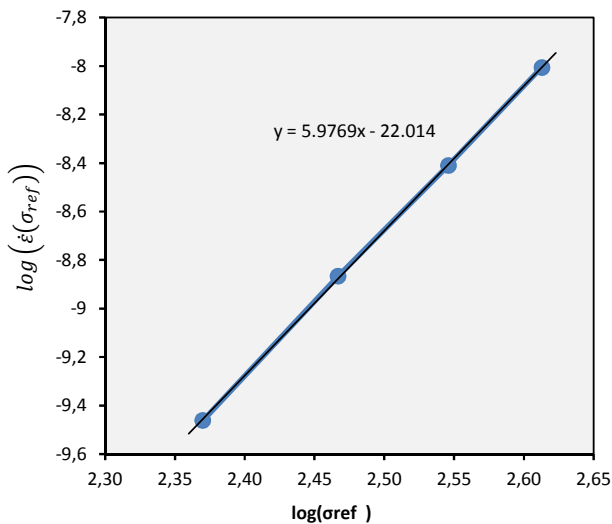

Fig. 9 Log plot of equivalent uniaxial strain rate against the equivalent uniaxial stress, with the deformation rate and the load applied to the thin plate

According to the log plot of Norton's Law, the gradient of the straight line is *n* and the intersection is equal to Log (B). Thus, the derived material parameters of creep can be obtained, as shown in Table IV .

TABLE IV
DETERMINATION OF NORTON'S LAW USING SIMULATIVE DATA

Parameter	Derived result	Set value	Error (%)
n	5.9769	6	0.457%
Log (A)	-22.014	-22	0.06%
B	0.96829^{-22}	10^{-22}	3.17%

From Table IV, it can be seen that the equivalent stress exponent *n* (= 5.9769) derived from thin plate tests is almost the same as the theoretical value (= 6), which gives an error of 0.457%. The derived Log (B) however has an error of 0.06% compared to the theoretical value. The error is reasonable for a power function, where a tiny change of stress will lead to a significant error. The differences between the values will account for the errors from empirical solutions.

V. DISCUSSION AND FUTURE WORK

As mentioned before, there is a strong need for the use of miniaturised specimens to determine the bulk creep properties at high temperature from a very small amount of material. The thin plate specimen provides an excellent alternative to other existing specimen types with some unique advantages. They are easier to be manufactured than all other existing small specimen types, due to their simplest geometry. More importantly, data obtained can be easily and accurately converted to the corresponding uniaxial data, since the majority part of the specimen is under a "uniaxial" stress state, due to "pure" bending. In particular, the specimen dimension in the thickness direction is very small, which is a significant advantage over some other small specimen types, such as impression creep specimen, for the situations when miniature specimens are needed to be removed from very narrow regions, such as the various microstructure regions of a heat affected zone in a power plant main steam pipe weld [5].

The analytical solution of the creep behaviour of beams under secondary and tertiary creep has been investigated previously [16]. In the present work, analytical solutions for the steady-state creep behaviour, i.e. the steady-state creep load-line deformation rates, of a thin plate, subjected to three-point bending, were obtained, in which the effects of shear stresses are not considered; for the geometry and loading used this is an acceptable assumption as shear effects would be practically negligible [17]. In practice, both creep strain rate and rupture data are expected to be obtained from such a test. In this paper, on the basis of Norton's Law, the analytical solutions for steady-state creep deformation rates are derived under plane-stress (very small *b*) and plane-strain (*b*→∞) conditions using a complementary strain energy approach. An approximate, empirical solution was then obtained for a range of *b/l* and *n* values of the plate, based on the results obtained from FE analyses. Based on this, the conversion relationships between the applied load and the equivalent uniaxial stress and between the steady-state creep deformation rate of thin plate and the equivalent uniaxial creep strain are established by the reference stress method. Using these relationships, it has been demonstrated that the creep properties obtained from thin plate simulative tests are in very good agreement with the theoretical values.

Future work will be carried out to produce the experimental test results in order to fully verify the conversion relationships developed. In addition, the data interpretation method should be modified to include the data conversion of creep rupture life time, if possible.

APPENDICES

A. Analytical Solutions under Plane Stress Conditions

A thin rectangular plate with simple supports subjected to a vertical point load P in the middle is illustrated in Fig. 2. Since

the plate is thin, the effect of the shear stress is assumed to be negligible. Under the plane stress, pure bending conditions, the plate is treated as a beam. For materials which creep based on Norton's law, the bending moment can be expressed as,

$$M = \frac{1}{B^{\frac{1}{n}}} \int y (\dot{K}y)^{\frac{1}{n}} dA \qquad (15)$$

If I_n is a plate area property

$$I_n = \int y^{1+\frac{1}{n}} dA \qquad (16)$$

then combining (15) and (16) leads to

$$M = \left(\frac{\dot{K}}{B}\right)^{\frac{1}{n}} I_n \ and \ \sigma^n = \frac{My^{\frac{1}{n}}}{I_n}$$

The complementary strain energy density u is

$$u = \int \varepsilon d\sigma = \frac{B}{n+1} |\sigma|^{n+1}$$

Therefore, the total complementary strain energy U of the plate is given by

$$U = \int u dV = \frac{2B}{(n+1){I_n}^n} \int_0^{l/2} |M|^{n+1} dx \qquad (17)$$

where V is volume of the thin plate. The moment M in the left part of the specimen is given by

$$M = \frac{P}{2} x \ (0 < x < \frac{L}{2})$$

Substituting the above into (17) gives

$$U = \frac{BL^{n+2}P^{n+1}}{4^{n+1}(n+1)(n+2){I_n}^n} \qquad (18)$$

By differentiating (18) with respect to the applied load P, the steady-state, load-line deformation rate $\dot{\Delta}_{ss}^c$ can be obtained

$$\dot{\Delta}_{ss}^c = \frac{dU}{dP} = \frac{BL^{n+2}P^n}{4^{n+1}(n+2){I_n}^n}$$

where I_n for a rectangular cross-section is in the form of

$$I_n = \frac{2nb}{2n+1} \cdot \left(\frac{d}{2}\right)^{2+\frac{1}{n}}$$

thus, the equation under the plane stress conditions is:

$$\dot{\Delta}_{ss}^c = \left(\frac{2n+1}{2n}\right)^n \frac{1}{2(n+2)} \cdot \frac{l^2}{d} \cdot B \left(\frac{Pl}{bd^2}\right)^n \qquad (19)$$

B. Analytical Solutions under Plane Strain Conditions

As shown in Fig. 3, a thin plate with simple supports is subjected to a vertical line load $\bar{p}$ in the middle. Since the plate is thin, the effect of the shear stress is assumed to be negligible, and the stress in the z direction is also negligible, under the plane strain conditions,

$$\sigma_z = 0$$
$$\varepsilon_y = 0$$

Using the relationships and the Hooke's Law, the stresses in x and y directions are related by:

$$\sigma_y = v\sigma_x \qquad (20)$$

where v is Poisson's Ratio.

In order to obtain the deformation rate of the thin plate under the plane strain conditions, a multi-axial form of creep behavior needs to be used. For a Norton's law, the effective stress is:

$$\sigma_{eff} = \frac{1}{\sqrt{2}} \sqrt{(\sigma_x - \sigma_y)^2 + (\sigma_x - \sigma_z)^2 + (\sigma_y - \sigma_z)^2}$$

Substituting the stress conditions into the above gives:

$$\sigma_{eff} = \sigma_x \sqrt{1 - v + v^2} \qquad (21)$$

The strain in the x direction under the effective stress is given by:

$$\varepsilon_x^c = \frac{B(\sigma_{eff})^n}{\sigma_{eff}} \left[\sigma_x - \frac{1}{2}(\sigma_y + \sigma_z)\right] \qquad (22)$$

Using (20) and with $\sigma_z = 0$, (22) can be simplified to:

$$\varepsilon_x^c = \frac{B(\sigma_{eff})^n}{\sigma_{eff}} \left(1 - \frac{v}{2}\right) \sigma_x \qquad (23)$$

Substitute (21) into (23) and thus creep strain in x direction is obtained:

$$\varepsilon_x^c = \left(1 - \frac{v}{2}\right) B (1 - v + v^2)^{\frac{n-1}{2}} {\sigma_x}^n \qquad (24)$$

For steady-state creep due to the volume assumption, the Poisson's ratio v takes a value of 0.5. Thus, (24) can be re-written to:

$$\varepsilon_x^c = \frac{3^{\frac{n+1}{2}}}{4} \cdot B{\sigma_x}^n \qquad (25)$$

Equation (25) is similar to Norton's law, and thus this equation can be used to obtain the deformation rate of thin plate under the plane strain conditions using the same method in Appendix A. The equation under the plane strain conditions is therefore given by:

$$\dot{\Delta}_{ss}^c = \left(\frac{2n+1}{2n}\right)^n \frac{1}{2(n+2)} \cdot \frac{l^2}{d} \cdot \frac{3^{\frac{n+1}{2}}}{4} \cdot B \left(\frac{\bar{p}l}{d^2}\right)^n \qquad (26)$$

NOMENCLATURE

b, d	cross-section dimensions of the plate
B, n	constants in Norton's creep law ($\dot{\varepsilon}^c = B\sigma^n$)
E, v	Young's modulus and Poisson's ratio
EGL	equivalent gauge length
I	second moment of area of the plate

I_n	cross-section property of the plate
$K, \dot{K}$	curvature and curvature rate
l	span of the supports of the thin plate
M	bending moment
$\bar{p}, P$	force per unit length and force
t	time
u, U	complementary strain energy density and complementary strain energy
V	volume
x, y, z	Cartesian coordinats
α	reference stress scaling factor
β, η	conversion factors
$\dot{\Delta}, \dot{\Delta}^c, \dot{\Delta}^c_{ss}$	deformation rate, creep deformation rate and steady state creep deformation rate, respectively
$\dot{\varepsilon}, \dot{\varepsilon}^c, \dot{\varepsilon}^c_{eq}$	strain rate, creep strain rate and equivalent creep strain rate, respectively
$\varepsilon_x, \varepsilon_y, \varepsilon_z$	strains in Cartesian coordinates
$\sigma, \sigma_1, \sigma_{eq}$	stress, maximum principal stress and equivalent stress, respectively
$\sigma_{nom}, \sigma_{ref}$	nominal stress and reference stress
$\sigma_x, \sigma_y, \sigma_z$	stresses in Cartesian coordinates

REFERENCES

[1] Hyde T. H., Sun W. and Williams J. A. The requirements for and the use of miniature test specimens to provide mechanical and creep properties of materials: - a review. *Int. Mater. Rev.* 52 (4), 213-255, 2007.

[2] Sun W., Hyde T. H. and Brett S. J. Small specimen creep testing and application for power plant component remaining life assessment. *4th Int. Conf. on Integrity, Reliability and Failure*. Madeira, 23-27 June, 2013.

[3] Parker J. D. and James J. D. (1994) Creep behaviour of miniature disc specimens of low alloy steel, ASME, PVP 279, *Developments in a Progressing Technology*, 167-172.

[4] Sun W. and Hyde T. H. Power plant remaining life assessment using small specimen testing techniques. *9th Annual Conf. on Operational Outages for Power Generation*. 28-30 March, 2011, Amsterdam, The Netherlands.

[5] Hyde T., Sun W., Becker A. A. and Williams J. Creep properties and failure assessment of new and fully repaired P91 pipe welds at 923 K. *Proc. Instn Mech. Engrs. Part L: J. Materials: Design and Applications* 218, 211-222, 2004.

[6] Askins M. C. and Marchant K. D. Estimating the remanent life of boiler pressure parts, EPRI Contract RP2253-1, Part 2, Miniature specimen creep testing in tension. CEGB Report. TPRD/3099/R86, CEGB, UK, 1987.

[7] Hyde T. H., Sun W. and Becker A. A. Analysis of the impression creep test method using a rectangular indenter for determining the creep properties in welds. *Int. J. Mech. Sci.*, 38, 1089-1102, 1996.

[8] Sun W., Hyde T. H. and Brett S. J. Application of impression creep data in life assessment of power plant materials at high temperatures. *Proc. Instn Mech. Engrs. Part L: J. Materials: Design and Applications* 222, 175-182, 2008.

[9] Li Y. Z. Determination of Norton creep law and rupture time dependence from small punch test. Proc. of *3rd Int. Conf. on Integrity of High Temp. Welds*, April 2007, IoM³ Communications, London, pp. 433-449, 2007.

[10] Rouse J. P., Cortellino F., Sun W., Hyde T. H., Shingledecker J. Small punch creep testing: a review on modelling and data interpretation. *Mater. Sci. Technol.* 29 (11), 1328-1345, 2013.

[11] Hyde T. H. and Sun W. A novel, high sensitivity, small specimen creep test. *J. Strain Analysis* 44 (3), 171-185, 2009.

[12] Sun W. and Hyde T. H. Determination of secondary creep properties using a small ring creep test technique. *Metallurgical Journal*, Vol. LXIII, 185-193, 2010.

[13] Balhassn A., Hyde T. H., Sun W. Analysis and design of a small, two-bar creep test specimen. *Trans. ASME J. Eng. Mater. & Technol.* 135 (4), 041006-1-041006-9, 2013.

[14] Fa-Kun Zhuang, Shan-Tung Tu, Guo-Yan Zhou and Qiong-Qi Wang. Assessment of creep constitutive properties from three-point bending creep test with miniaturized specimens. *J. Strain Analysis* 46, 1-10, 2014.

[15] MacKenzie A. C. On the use of a single uniaxial test to estimate deformation rates in some structures undergoing creep. *Int. J. Mech. Sci.* 10, 441-453, 1968.

[16] Altenbach H., Kolarow G., Morachkovsky O. K. and Naumenko K. On the accuracy of creep-damage predictions in thin walled structures using the finite element method. *Computational Mechanics* 25, 87-98, 2000.

[17] Altenbach H. and Naumenko K. Shear correction factors in creep damage analysis of beams, plates and shells. *JSME Int. Journal*, Series A 45 (1), 77-83, 2002.